Interaction Notes

Note 570

20 June 2001

Substructure SEM

Carl E. Baum
Air Force Research Laboratory
Directed Energy Directorate

Abstract

This paper discusses the problem of separating out the response of substructures on larger bodies from the full-body resonances which explicitly appear in the singularity expansion method (SEM). In some cases one can formulate the substructure scattering as a perturbation on the larger body viewed locally as a perfectly conducting plane. However, some important cases have the perturbation on or near edges for which allowance is needed in the Green function. There is an experimental application of such concepts as well, separating out the substructure resonances in the data processing.

This work was sponsored in part by the Air Force Office of Scientific Research, and in part by the Air Force Research Laboratory, Directed Energy Directorate.

1. Introduction

In recognizing (identifying) an object (target) from a scattered electromagnetic wave, various problems present themselves. Among these are low-frequency limitations on radars due to antenna size and associated beam width in transmission and reception. As a result many scatterers have their major linear dimensions large compared to the sensing wavelengths.

From the singularity expansion method (SEM) we have a target signature consisting of the aspect-independent natural frequencies (pole locations in the $s = \Omega + j\omega$ plane). For large scatterers the lower-frequency poles may then not be sufficiently excited to be useful for identification purposes. However, there are higher-order poles which may be in the frequency range of our radar.

The higher-order poles s_α of interest have the smaller damping constants ($-\Omega_\alpha$), i.e., are more resonant. These can be associated with substructures on the larger scatterer. By substructures let us think of these as local perturbations on a surface (perfectly conducting or otherwise) with larger characteristic dimensions. It is then of interest to have some perturbation techniques to develop the SEM representation of such substructures. This applies not only to the scattering theory, but also to the data-processing techniques to be used to identify the presence of such substructure resonances.

2. Protrusion on Perfectly Conducting Ground Plane

A simple form of substructure is something on (or near) a perfectly conducting plane, since it allows to use image theory. Figure 2.1 shows the example of a perfectly conducting boss on this ground plane denoted by surface S_b. Its image is denoted by S_i and we define

$$S \equiv S_b \cup S_i \tag{2.1}$$

The response of the boss is found by the response of S to the incident wave plus its image in the ground plane.

The incident fields are given by

$$\tilde{\vec{E}}^{(inc)}(\vec{r},s) = E_0 \tilde{f}(s) e^{-\gamma \vec{1}_i \cdot \vec{r}} \vec{1}_e$$

$$\tilde{\vec{H}}^{(inc)}(\vec{r},s) = \frac{E_0}{Z_0} \tilde{f}(s) e^{-\gamma \vec{1}_i \cdot \vec{r}} \vec{1}_i \times \vec{1}_e$$

$\vec{1}_i \equiv$ direction of incidence

$\vec{1}_e \equiv$ polarization , $\vec{1}_i \cdot \vec{1}_e = 0$

$\sim \equiv$ two-sided Laplace transform over time t

$s = \Omega + j\omega \equiv$ Laplace-transform variable or complex frequency

$\gamma = \frac{s}{c} \equiv$ propagation constant (2.2)

$c = [\mu_0 \varepsilon_0]^{-\frac{1}{2}} \equiv$ speed of light

$Z_0 = \left[\frac{\mu_0}{\varepsilon_0}\right]^{\frac{1}{2}} \equiv$ wave impedance of free space

$f(t) =$ waveform

Note that the polarization is some combination of the usual radar polarizations $\vec{1}_h$ and $\vec{1}_v$ indicated in Fig. 2.1. To this we need to add reflected fields

$$\tilde{\vec{E}}^{(refl)}(\vec{r},s) = E_0 \tilde{f}(s) e^{-\gamma \vec{1}_i' \cdot \vec{r}} \vec{1}_e'$$

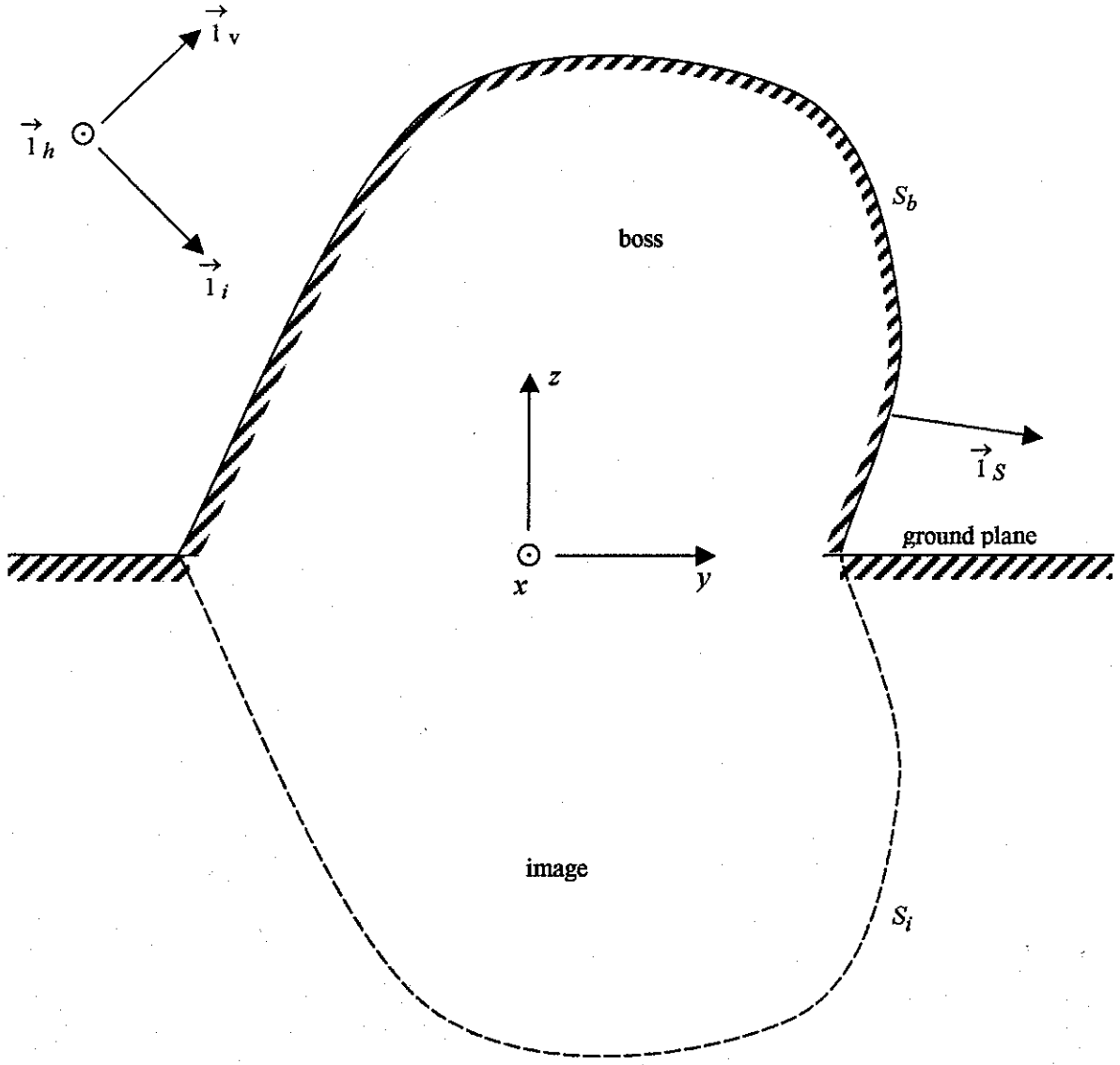

Fig. 2.1 Boss on Perfectly Conducting Ground Plane

$$\tilde{\vec{H}}^{(refl)}(\vec{r},s) = E_0\,\tilde{f}(s)e^{-\gamma\,\vec{1}'_i\cdot\vec{r}}\,\vec{1}'_i\times\vec{1}'_e$$

$$\vec{1}'_i = \overleftrightarrow{R}_z\cdot\vec{1}_i$$

$$\vec{1}'_e = -\overleftrightarrow{R}_z\cdot\vec{1}_e$$

$$\overleftrightarrow{R}_z = \overleftrightarrow{1} - 2\vec{1}_z\vec{1}_z = \begin{pmatrix}1&0&0\\0&1&0\\0&0&-1\end{pmatrix} \equiv \text{reflection dyadic} \tag{2.3}$$

$$\overleftrightarrow{1} = \vec{1}_x\vec{1}_x + \vec{1}_y\vec{1}_y + \vec{1}_z\vec{1}_z = \begin{pmatrix}1&0&0\\0&1&0\\0&0&1\end{pmatrix} \equiv \text{three dimensional identity}$$

Note that on the ground plane the sum of the tangential incident and reflected electric fields is zero. This is an example of an antisymmetric field distribution (including images) [10].

We can find the surface current density from the impedance or E-field integral equation as [1]

$$\left\langle \tilde{\overleftrightarrow{Z}}_t(\vec{r}_s,\vec{r}'_s;s);\ \tilde{\vec{J}}_s(\vec{r}'_s,s)\right\rangle = \tilde{\vec{E}}_t^{(inc)}(\vec{r}_s,s) + \tilde{\vec{E}}_t^{(refl)}(\vec{r}_s,s)$$

$$= \overleftrightarrow{1}_S(\vec{r}_s)\cdot\left[\tilde{\vec{E}}^{(inc)}(\vec{r}_s,s) + \tilde{\vec{E}}^{(refl)}(\vec{r}_s,s)\right]$$

$$\vec{r}_s,\vec{r}'_s \in S$$

$$\overleftrightarrow{1}_S(\vec{r}_s) = \overleftrightarrow{1} - \vec{1}_S(\vec{r}_s)\vec{1}_S(\vec{r}_s)$$

$$\vec{1}_S(\vec{r}_s) \equiv \text{unit normal (outward to } S)$$

$$\tilde{\overleftrightarrow{Z}}_t(\vec{r}_s,\vec{r}'_s;s) = \overleftrightarrow{1}_S(\vec{r}_s)\cdot\tilde{\overleftrightarrow{Z}}(\vec{r}_s,\vec{r}_s;s)\cdot\overleftrightarrow{1}_S(\vec{r}'_s)$$

$$= s\mu_0\overleftrightarrow{1}_S(\vec{r}_s)\cdot\tilde{\overleftrightarrow{G}}_0(\vec{r}_s,\vec{r}'_s;s)\cdot\overleftrightarrow{1}_S(\vec{r}'_s)$$

$$= \frac{Z_0\gamma^2}{4\pi}\overleftrightarrow{1}_S(\vec{r}_s)\cdot\left[\left[-2\zeta^{-3}-2\zeta^{-2}\right]e^{-\zeta}\vec{1}_R\vec{1}_R + \left[\zeta^{-3}+\zeta^{-2}+\zeta^{-1}\right]e^{-\zeta}\left[\overleftrightarrow{1} - \vec{1}_R\vec{1}_R\right]\right]\cdot\overleftrightarrow{1}_S(\vec{r}'_s)$$

$$R = |\vec{r}_s - \vec{r}'_s|\ ,\quad \zeta = \gamma R$$

$$\vec{1}_R = \frac{\vec{r}_s - \vec{r}'_s}{|\vec{r}_s - \vec{r}'_s|} \quad \text{for } \vec{r}_s \neq \vec{r}'_s \tag{2.4}$$

where integration is over all of S as in (2.1). The natural frequencies and modes are found from

$$\left\langle \overleftrightarrow{Z}_t(\vec{r}_s, \vec{r}'_s; s); \vec{j}_{s_\alpha}(\vec{r}'_s) \right\rangle = \vec{0}$$

$$s_\alpha \equiv \Omega_\alpha + j\omega_\alpha \equiv \text{natural frequency} \tag{2.5}$$

$$\vec{j}_{s_\alpha}(\vec{r}_s) \equiv \text{natural mode}$$

These are aspect independent (independent of the incident plus reflected field). While the computation is over S, we need to restrict solutions of (2.5) to antisymmetric modes for which

$$\vec{j}_{s_\alpha}(\overleftrightarrow{R}_s \cdot \vec{r}_s) = -\overleftrightarrow{R}_z \cdot \vec{j}_{s_\alpha}(\vec{r}_s) \tag{2.6}$$

Furthermore, we need to reject solutions for s_α on the $j\omega$ axis as internal (to S) cavity resonances.

The case of a perfectly conducting boss on a perfectly conducting ground plane is then a relatively simple form of substructure, which readily lends itself to SEM analysis. The ground plane contributes no natural frequencies other than in forming the image of the boss. Of course, infinite perfectly conducting ground planes do not exist in practice. In time domain, however, we have a time separation (clear time) between the arrival of the incident wave and the arrival of scattering from the ground-plane edges at the boss. While the formulation here is for a flat ground plane, the solution should approximately apply to a curved surface approximating the ground plane in the vicinity of the boss. The magnitudes of the principal radii of curvature of this surface should be large compared to the characteristic dimensions of the boss.

3. Indentation in Perfectly Conducting Ground Plane

Unlike the protrusion above the ground plane the case of the depression below a ground plane does not allow for a simple analysis by image theory. Figure 3.1 shows the example of a perfectly conducting bowl in this ground, now defined by surface S_b. The hole in the ground plane is denoted by S_c on the $z = 0$ plane connecting the exterior world to the bowl.

This problem can be formulated in terms of integrals over $S_b \cup S_c$ for the bowl and over S_c with a half-space Green function. Without going into details, it has been shown [6] that one can formulate an integral equation over S_b only for the surface current density on the bowl. For this purpose we need scalar Green functions

$$\begin{aligned}
\tilde{G}(\vec{r},\vec{r}';s) &= \frac{e^{-\gamma|\vec{r}-\vec{r}'|}}{4\pi|\vec{r}-\vec{r}'|} = \tilde{G}(\vec{r}',\vec{r};s) \\
\tilde{G}_D(\vec{r},\vec{r}';s) &= \tilde{G}(\vec{r},\vec{r}';s) - \tilde{G}(\vec{r},\vec{r}'_m;s) \\
\tilde{G}_N(\vec{r},\vec{r}';s) &= \tilde{G}(\vec{r},\vec{r}';s) + \tilde{G}(\vec{r},\vec{r}'_m;s) \\
\vec{r}_m &= \overleftrightarrow{R}_z \cdot \vec{r}
\end{aligned} \tag{3.1}$$

with this we form a dyadic Green function

$$\begin{aligned}
\tilde{\overleftrightarrow{\Gamma}}(\vec{r},\vec{r}';s) &= \gamma\nabla\times\left[\tilde{G}_D(\vec{r},\vec{r}';s)\,\overleftrightarrow{1}_z + \tilde{G}_N(\vec{r},\vec{r}';s)\,\vec{1}_z\,\vec{1}_z\right] \\
&= -\tilde{\overleftrightarrow{\Gamma}}(\vec{r}',\vec{r};s) \\
\overleftrightarrow{1}_z &= \vec{1}_x\,\vec{1}_x + \vec{1}_y\,\vec{1}_y
\end{aligned} \tag{3.2}$$

The surface current density on the shorted aperture S_c is

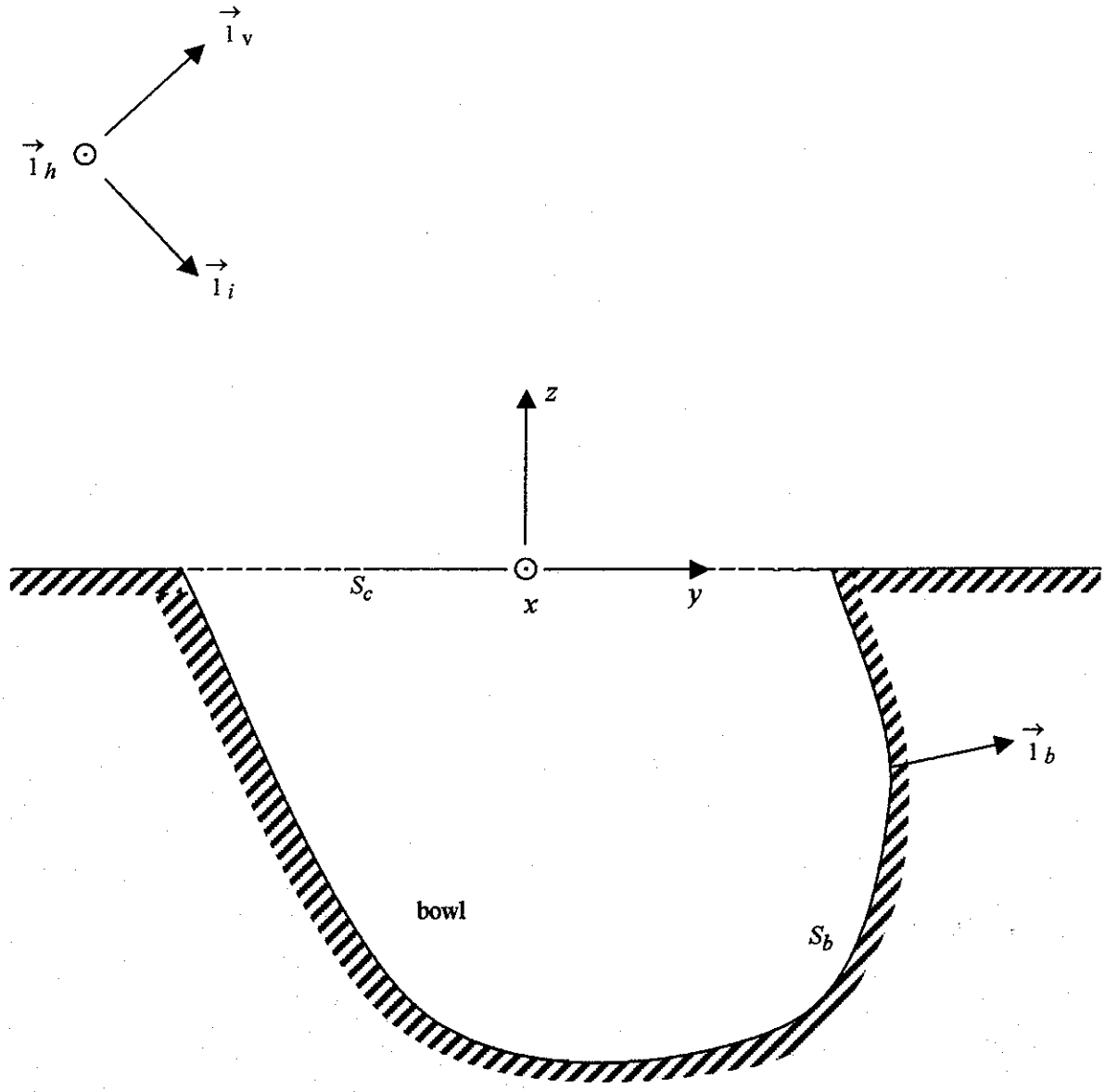

Fig. 3.1 Bowl in Perfectly Conducting Ground Plane

$$
\begin{aligned}
\tilde{\vec{J}}_s^{(0)}(\vec{r}_s,s) &= \vec{1}_z \times \tilde{\vec{H}}^{(0)}(\vec{r}_s,s) \\
\tilde{\vec{H}}^{(0)}(\vec{r}_s,s) &= \vec{1}_z \cdot \left[\tilde{\vec{H}}^{(inc)}(\vec{r}_s,s) + \tilde{\vec{H}}^{(refl)}(\vec{r}_s,s) \right] \\
&= 2\,\overleftrightarrow{1}_z \cdot \tilde{\vec{H}}^{(inc)}(\vec{r}_s,s) \\
\vec{r}_s &\in S_c
\end{aligned}
\tag{3.3}
$$

From this a source term for the integral equation is formed as

$$
\tilde{\vec{F}}(\vec{r}_s,s) = \vec{1}_b(\vec{r}_s) \times \left[\int_{S_c} \left[\nabla' \tilde{G}(\vec{r}_s,\vec{r}'_s;s) \Big|_{\vec{r}'=\vec{r}'_s} \right] \times \tilde{\vec{J}}(\vec{r}'_s,s)\,dS'_c \right]
\tag{3.4}
$$

$$
\vec{r}_s \in S_b \quad , \quad \vec{r}'_s \in S_c \quad \text{(integrated out)}
$$

The integral equation over S_b takes the form

$$
\frac{1}{2}\tilde{\vec{J}}(\vec{r}_s,s) + \left\langle \tilde{\overleftrightarrow{X}}(\vec{r}_s,\vec{r}'_s;s)\, \tilde{\vec{J}}_s(\vec{r}'_s,s) \right\rangle = \tilde{\vec{F}}(\vec{r}',s)
\tag{3.5}
$$

$$
\vec{r}_s, \vec{r}'_s \in S_b
$$

with integration now only over $\vec{r}'_s$ on S_b. The kernel is

$$
\begin{aligned}
\tilde{\overleftrightarrow{X}}(\vec{r}_s,\vec{r}'_s;s) &= -\frac{1}{\gamma}\overleftrightarrow{1}_b(\vec{r}_s) \times \tilde{\overleftrightarrow{\Gamma}}(\vec{r}_s,\vec{r}'_s;s) \\
&+ 2\int_{S_c} \left[\left[\nabla' \tilde{G}(\vec{r}',r''_s;s) \Big|_{\vec{r}'=r'_s} \right] \times \left[\left[\vec{1}_z \times \overleftrightarrow{1} \right] \left[\vec{1}_b(\vec{r}_s) \cdot \nabla \tilde{G}(\vec{r},\vec{r}''_s;s) \Big|_{\vec{r}=\vec{r}_s} \right] \right. \right. \\
&\left. \left. + \left[\vec{1}_b(\vec{r}_s) \times \vec{1}_z \right] \left[\nabla \tilde{G}(\vec{r},\vec{r}''_s;s) \Big|_{\vec{r}=\vec{r}_s} \right] \right] \right] dS''_c
\end{aligned}
\tag{3.6}
$$

$$
\vec{r}_s, \vec{r}'_s \in S_b \quad , \quad \vec{r}''_s \in S_c \quad \text{(integrated out)}
$$

Natural frequencies and modes are then found from

$$\frac{1}{2}\vec{j}_{s_\alpha}(\vec{r}_s) + \left\langle \overleftrightarrow{\tilde{X}}(\vec{r}_s, \vec{r}'_s; s); \vec{j}_{s_\alpha}(\vec{r}'_s) \right\rangle = \vec{0} \qquad (3.7)$$

$$\mathrm{Re}[s_\alpha] = \Omega_\alpha < 0$$

similar to (2.5). Again the perfectly conducting ground plane contributes no natural frequencies of its own. As in Section 2 a curved ground plane, with radii of curvature large compared to the characteristic dimensions of the bowl, will still allow (3.7) to give a good approximation.

The reader can note that there are yet other ways to formulate the problem, suitable for numerical solution [4].

4. Protrusion Near an Edge

The more general case has a protrusion (or boss) on a nonflat perfectly conducting surface. Suppose that the ground plane is bent to form a wedge as in Fig. 4.1. The Green function for a wedge is quite different from that for an infinite plane [9 (ch. 9)], even in the limiting case of a half plane. While not a resonant structure there is a branch cut in the complex frequency plane.

As in Fig. 4.1A we may have a boss sufficiently far from the edge (compared to the boss size) that locally the boss resonances may be analyzed as an infinite perfectly conducting ground plane. However, as in Fig. 4.1B and C, if the protrusion is near or even on the edge the problem is essentially different. The Green function for the wedge represents the fields resulting from a current element near (but outside) this edge. Varying the position of this current element over the surface S_p of this protrusion, and setting the tangential electric field there to zero gives an integral equation similar to (2.1). Setting the incident field to zero gives an equation like (2.5) for the natural frequencies and modes. However, there is the complication of the branch cut with which to contend. As usual the internal (cavity) resonances are excluded.

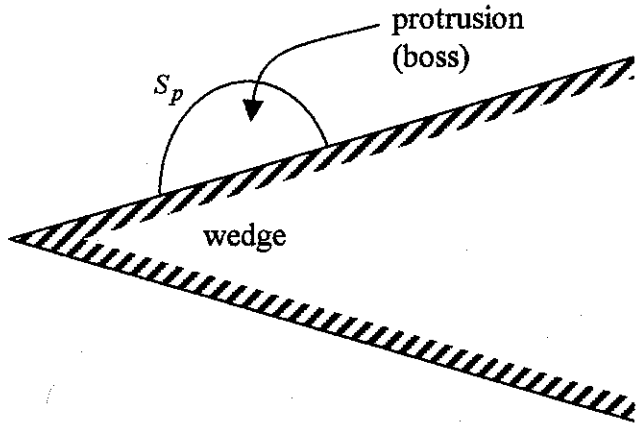

A. Protrusion not too close to edge

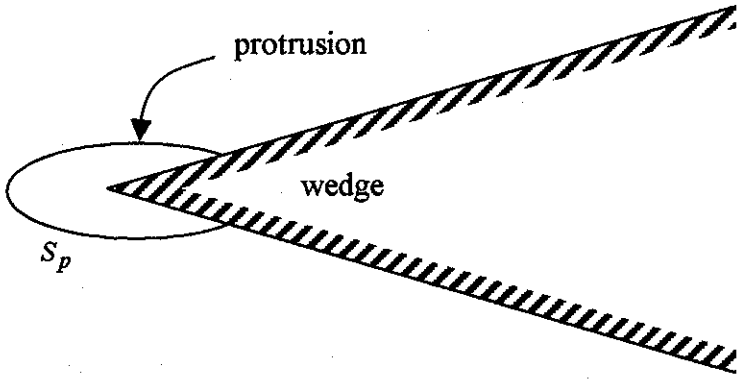

B. Protrosion on edge: view along edge

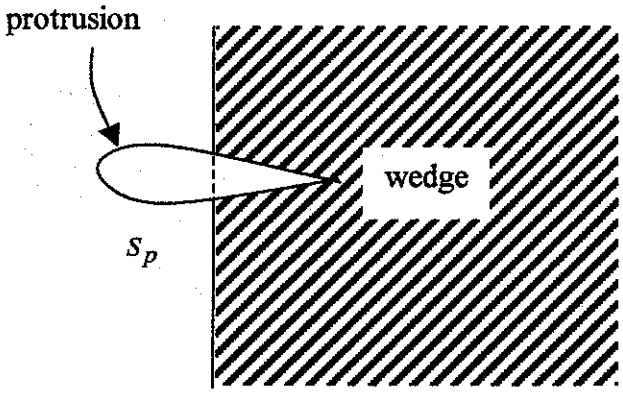

C. Protrusion on edge: view perpendicular to edge

Fig. 4.1 Protrusion Near an Edge

5. Separating Substructure Resonances from Full-Body Resonances

From a target-recognition point of view one would like to consider the substructure natural frequencies separately from the lower-frequency full-body resonances. An isolated scatterer has an SEM response characterized by a scattering dyadic, which for backscattering has the form [1, 3]

$$\overleftrightarrow{\Lambda}_b(\vec{1}_i,s)=\sum_\alpha \frac{e^{-[s-s_\alpha]t_p}}{s-s_\alpha}\vec{c}_\alpha(\vec{1}_i)\vec{c}_\alpha(\vec{1}_i) + \text{entire function}$$

$$\overleftrightarrow{\Lambda}_b(\vec{1}_i,t)=\sum_\alpha e^{s_\alpha t}u(t-t_p)\vec{c}_\alpha(\vec{1}_i)\vec{c}_\alpha(\vec{1}_i) + \text{entire function (temporal form)} \qquad (5.1)$$

$\vec{1}_i \equiv$ direction of incidence

$t_p \equiv$ turn-on time, typically retarded time of first signal return to observer

As discussed in [1, 3] the scattering generally does have an entire-function contribution. In time domain this is an early time contribution. Just when is late time so that only complex exponentials need to be considered is now reasonably well understood.

For simplicity let us assume that the substructure of interest is on the illuminated side of the target. This lets us model the source field for the protrusion as $\vec{E}^{(inc)} + \vec{E}^{(refl)}$ as in Section 2, at least for times before scattering from other parts of the full body reaches the substrcture. (If the substructure is in the shadow region, then creeping waves and diffracted waves assume the role of the incident field at the substructure.) Then, deconvolving the incident-field waveform to obtain the delta- or step-function response, let us think of the backscattering as the sum of the substructure response in the form of (5.1) plus the response due to the larger body on which the substructure resides.

In scalar form a measurement will take the form

$$f(t) = f_s(t) + f_f(t)$$
$$f_s(t) = \sum_\alpha R_\alpha e^{s_\alpha t}u(t-t_p) + \text{entire function (temporal form)}$$
$$\equiv \text{substructure response} \qquad (5.2)$$

$f_f(t) \equiv$ full-body response

What form should $f_f(t)$ take? While we don't wish to make a detailed model, let us look for some general form that will be valid during the important times in the late time of $f_s(t)$, i.e., after the entire function (temporal form) is over, and including after the identification time (the first time signal returns from the farthest part of the substructure).

As an approximation let us assume that the full-body response is slowly varying during the important sub-structure-response times. This is certainly the case for the dominant low-frequency resonances of the full body. If there are higher order resonances of the full body or significant scattering from other substructures, we assume for present purposes that they are not significant during the time window for identifying the particular substructure of interest.

For this slowly varying background let us assume that it can be well approximated during the time window of interest by a series of the form

$$f_f(t) = \sum_{n=0}^{\infty} f_n \left[t - t_f \right]^n \tag{5.3}$$

where we will use only the first few terms and t_f is chosen at our convenience (say at the beginning of, or in the middle of, the time window).

The problem then is to fit the exponentials for f_s plus a few terms of f_f to the measured (deconvolved) data. An important current approach to this is the matrix pencil [7] which is gaining more accuracy, but currently only includes the exponential terms. In principle one can take, say the first three terms from (5.3), add these to the f_s series for a least square fit. By shifting the time window and insisting that the same functions and coefficients apply to all the time windows, perhaps the matrix-pencil technique can be generalized in this form as well. This is a potential direction for future research.

6. Implications for ξ-Pulse

An alternate procedure for target discrimination uses a filter on the data to remove the late time resonances if the proper target is selected from a library. This goes by various names including E-pulse, K-pulse, and ξ-pulse [2, 5, 8]. Convolving such a temporal pulse for each target in the library with the data one looks for the minimum late time residual to choose the correct target.

Beginning with an elementary pulse (annihilation pulse)

$$\begin{aligned} a_\ell(t) &= \delta(t) - e^{s_\ell T_0}\delta(t) \\ T_0 &\equiv \text{sampling interval in time} \\ s_\ell &\equiv \ell\text{th natural frequency} \end{aligned} \tag{6.1}$$

one forms a ξ-pulse as

$$\begin{aligned} \xi(t) &= a_1(t) \circ a_2(t) \circ \cdots \circ a_L(t) \\ \xi(t) \circ &= \prod_{\ell=1}^{L} [a_\ell(t) \circ] \\ \circ &\equiv \text{convolution with respect to time } t \end{aligned} \tag{6.2}$$

These convolutions give closed analytic forms for $\xi(t)$. Here L can be even or odd including both conjugate pole pairs and poles on the negative real axis of the s plane.

Applying this to (5.2) gives

$$g(t) = \xi(t) \circ f(t) = \xi(t) \circ f_S(t) + \xi(t) \circ f_f(t) \tag{6.3}$$

If $\xi(t)$ corresponds to the correct target then

$$\xi(t) \circ f_S(t) \simeq 0 \tag{6.4}$$

at late times (after the entire function plus width of $\xi(t)$) noting that practically only a finite number of the s_ℓ can be included. This then leaves at late times

$$g(t) \simeq \xi(t) \circ f_f(t) \tag{6.5}$$

Expanding $g(t)$ similarly to (5.3) gives

$$g(t) \simeq \sum_{n=0}^{\infty} g_n \left[t - t_f\right]^n \tag{6.6}$$

Now one can take the first few of these to approximate the full-body response (filtered by $\xi(t)$) during the time window of interest. One can choose g_0, g_1, and perhaps g_2 based on certain moments of the data, or such that the rms value of $g(t)$ less these terms is minimized to form some kind of corrected residual. Comparing the corrected residuals using the $\xi(t)$ for the various targets in the library then leads to the target choice with the smallest corrected residual.

An alternate procedure uses a discrete derivative operator

$$\begin{aligned} b(t)\circ &= \left[\delta(t) - \delta(t - T_f)\right]\circ \\ T_f &= \text{integer multiple of } T_0 \quad (1, 2, \ldots) \end{aligned} \tag{6.7}$$

Applying this to a term in (6.6), we have

$$\begin{aligned} b(t)\circ\left[t - t_f\right]^n &= \left[t - t_f\right]^n - \left[t - t_f - T_f\right]^n \\ &= nT_f\left[t - t_f\right]^{n-1} - \frac{n[n-1]}{2}T_f^2\left[t - t_f\right]^{n-2} \\ &\quad + \cdots - \left[-T_f\right]^n \quad \text{for } n = 1, 2, \cdots \\ b(t)\circ\left[t - t_f\right]^0 &= 0 \end{aligned} \tag{6.8}$$

Applying the operator successively we note that

$$\left[b(t)\circ\right]^{n+1}\left[t - t_f\right]^n = 0 \tag{6.9}$$

So, if we take n = 0, 1, ..., N terms in (6.6) we have

$$\left[b(t)\circ\right]^{N+1}\left[\sum_{n=0}^{N} g_n\left[t-t_f\right]^n\right] = 0 \tag{6.10}$$

and we do not need to compute $g_0, g_1, \cdots, g_N$.

With the $\xi(t)$ chosen for the correct target then we expect

$$\left[b(t)\circ\right]^{N+1}\circ g(t) = \left[b(t)\circ\right]^{N+1}\xi(t)\circ f_f(t) \tag{6.11}$$

to be small. However, when applied to the total data with $\xi(t)$ chosen for the wrong target we have

$$\left[b(t)\circ\right]^{N+1}\circ g(t) = \left[b(t)\circ\right]^{N+1}\circ\xi(t)\circ f_s(t) + \left[b(t)\circ\right]^{N+1}\circ\xi(t)\circ f_f(t) \tag{6.12}$$

Looking at the first term we see that the discrete derivative operator also operates on $f_s(t)$, changing the residual in the case of an incorrectly chosen target. This should still be nonzero, but allowance needs to be made for this.

There is some flexibility in our choice of T_f. It can be as small as our basic sampling interval T_0, but one may elect some number of sampling intervals if this gives better performance.

7. Concluding Remarks

This is just a beginning on the subject of substructure SEM. It would be helpful to have calculations for various canonical substructures. Equally important are the data processing algorithms for experimental implementation.

I would like to thank L. Carin and J.-M. Jin for discussions and assistance in locating some of the references.

References

1. C. E. Baum, "Representation of Surface Current Density and Far Scattering in EEM and SEM with Entire Functions," Interaction Note 486, February 1992; ch. 13, pp. 273-316, in P. P. Delsanto and A. W. Saenz (eds.), *New Perspectives on Problems in Classical and Quantum Physics, Part II, Acoustic Propagation and Scattering, Electromagnetic Scattering*, Gordon and Breach, 1998.

2. C. E. Baum, "Direct Construction of a ξ-Pulse from Natural Frequencies and Evaluation of Late-Time Residuals," Interaction Note 519, May 1996; pp. 349-360, in E. Heyman, B. Mandelbaum, and J. Shiloh (eds.), *Ultra-Wideband, Short-Pulse Electromagnetics 4*, Kluwer Academic/Plenum Publishers, 1999.

3. C. E. Baum, "An Observation Concerning the Entire Function in SEM Scattering," Interaction Note 567, April 2001.

4. J.-M. Jin and J. L. Volakis, "A Finite Element—Boundary Integral Formulation for Scattering by Three-Dimensional Cavity-Backed Apertures," IEEE Trans. Antennas and Propagation, 1991, pp. 97-104.

5. C. E. Baum, E. J. Rothwell, K.-M. Chen, and D. P. Nyquist, "The Singularity Expansion Method and Its Application to Target Identification," Proc. IEEE, 1991, pp. 1481-1492.

6. J. S. Asvestas and R. E. Kleinman, "Electromagnetic Scattering by Indented Screens," IEEE Trans. Antennas and Propagation, 1994, pp. 22-30.

7. T. K. Sarkar, S. Park, J. Koh, and S. M. Rao, "Application of the Matrix Pencil Method for Estimating the SEM (Singularity Expansion Method) Poles of Source-Free Transient Responses from Multiple Look Directions," IEEE Trans. Antennas and Propagation, 2000, pp. 612-618.

8. J. E. Mooney, Z. Ding, and L. S. Riggs, "Performance Analysis of an Automated E-Pulse Target Discrimination Scheme," IEEE Trans. Antennas and Propagation, 2000, pp. 619-628.

9. C.-T. Tai, *Dyadic Green Functions in Electromagnetic Theory*, 2nd Ed., IEEE Press, 1994.

10. C. E. Baum and H. N. Kritikos, "Symmetry in Electromagnetics," ch. 1, pp. 1-90, in C. E. Baum and H. N. Kritikos (eds.), *Electromagnetic Symmetry*, Taylor & Francis, 1995.